Indian Institute of Science Education

and Research, Kolkata

Oxygen Evolution Reaction

(OER)

Name: Priyanshu Kumar

Student ID: 23MS080

Supervisor: Venkataramanan Mahalingam

Table of Content

[17/07/2025]

1. Abstract:

The Oxygen evolution reaction (OER) is a pivotal technology driving next generation sustainable energy conservation and storage devices.The development of efficient electrocatalysts to lower the overpotential of OER is fundamental importance in improving the overall efficiency and cost of fuel production by water electrocatalysis. Among a galore of catalysts, transition metal oxides/hydroxides exhibit reasonable activity and stability in alkaline electrolysis. OER mechanism under Acidic and alkaline conditions are quite different. Understanding OER for transition metal oxides/hydroxides in alkaline electrolyties paves the way for better design of low cost and highly efficient electrocatalysts. Substantial efforts have been devoted to understanding the factors that determine the OER activity and searching for activity descriptors. Different parameters have been studied throughout the years. With a better understanding of how material properties and dynamic environment influence the OER activity and mechanism,we can obtain more efficient OER catalysts for better energy infrastructure.

2. Introduction:

Problem Statement: Why OER?

As the time is progressing demand of energy consumption is increasing exponentially, conventional methods of energy like fossil fuels will not be able fulfill energy needs of future and they have also brought up severe environmental issues like pollution. Hence we need environment friendly sustainable energy sources to fulfill worldwide energy demand. Hydrogen is one of the green energy which can be used consistently in a clean way through electrolysis. Hydrolysis of reactive metals, metal hydrides and alkali and alkaline earth metal borohydrides is a relatively rapid method of producing hydrogen in large quantities. However, the sources are always toxic metals, metal hydrides and borohydrides that are synthesized via fine chemical industries on a large scale while polluting the environment.This means that this method can not be adopted as a greener way for producing large amount of Hydrogen. Hence water electrolysis is the best method to produce highly pure H_2 on a large scale within short periods of time and with much less harm to the environment.

The essential idea for this two electrode setup is Cathode part includes hydrogen evolution reaction (HER) or oxygen reduction reaction (ORR) and the anode part proceeds with oxygen evolution reaction (OER) or oxidation of some chemical fuels. The reason that keeps these systems impractical is the sluggish kinetics of OER. OER is a four electron-proton coupled reaction while HER is only a two electron-transfer reaction, hence anodic OER requires higher overpotential to overcome the kinetic barrier.
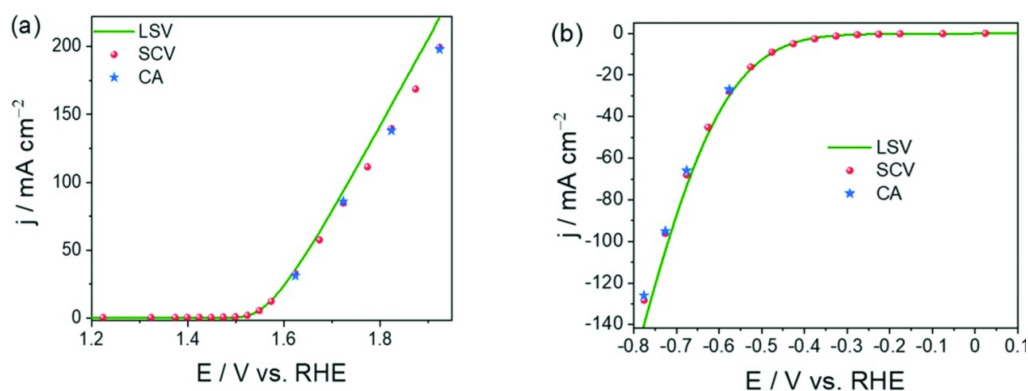
Fig: OER (a) and HER (b) polarization curves obtained using LSV and SCV and provided in comparison with the activity determined using CA.

3. Background for OER:

Overconsumption of fossil fuels has caused severe environmental issues. And fossil fuels can not meet the increasing energy demand worldwide anymore. Thus it is important to switch to clean energy sources that can be produced from sustainable sources. Hydrogen fuel is one of them. The advantage of water splitting is that it provides clean hydrogen without harming our environment.In this electrochemical process hydrogen evolves at cathode and oxygen evolves at anode.
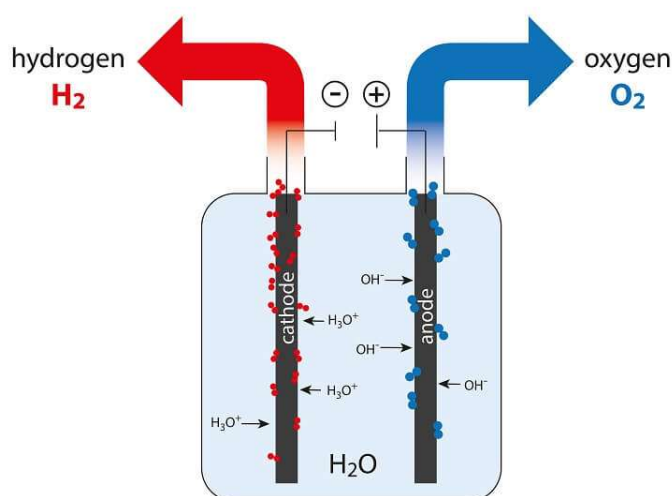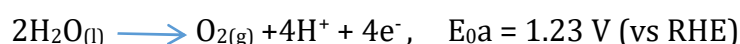

Fig: Schematic illustration of electrochemical water splitting

Below are the half reactions at both cathode and anode in acidic and alkaline conditions.
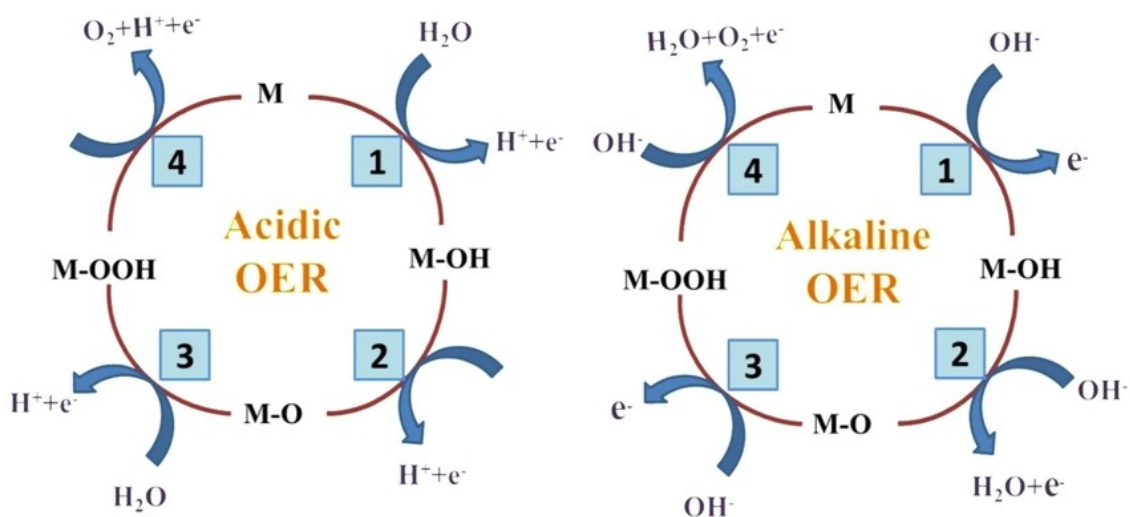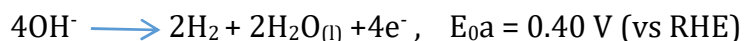
Acidic condition:

Cathode reaction:

$$4H_+ + 4e^- \longrightarrow 2H_2, \qquad E_0c = 0 \text{ V (vs RHE)}$$

Anode reaction:

$$2H_2O_{(l)} \longrightarrow O_{2(g)} + 4H^+ + 4e^-, \quad E_0a = 1.23 \text{ V (vs RHE)}$$

Alkaline conditions:

Cathode reaction:

$$4H_2O + 4e^- \longrightarrow 2H_2 + 4OH^-, \quad E_0c = 0.83 \text{ V (vs RHE)}$$

Anode reaction:

$$4OH^- \longrightarrow 2H_2 + 2H_2O_{(l)} + 4e^-, \quad E_0a = 0.40 \text{ V (vs RHE)}$$

The

Fig: Mechanistic steps involved in OER with four proton and four electron coupled electron transfer in acidic and alkaline electrolyte.

4. Performance Evaluation of a OER catalyst:

An electrocatalyst is the catalyst that is used to facilitate electrochemical reactions. The main function of a electrocatalyst is to absorb reactant on the surface to form absorbed intermediate and thereby facilitate charge transfer between the electrode and reactant.

There are mainly three electrochemical methods: cyclic voltammetry (CV), chronopotentiometry (CP), chronoamperometry (CA). There are a few electrochemical parameters which are used to fairly evaluate the performance of the electrochemical reactions such as overpotential (η), exchange current density (i_0), Tafel slope (b), turnover frequency (TOF), mass activity and specific activity.

4.1. Overpotential (η): In an ideal world, applied potential for driving a specific reaction should be equal to the potential of the reaction at equilibrium. In reality, it is always not the case. Applied potentail is much higher than the potentail at equilibrium. "the **extra voltage** (beyond the theoretical minimum) that must be applied to drive an electrochemical reaction at a measurable rate is called the overpotential".

$$E = E^{0'} + RT/nF * \ln(C_0/C_R)$$
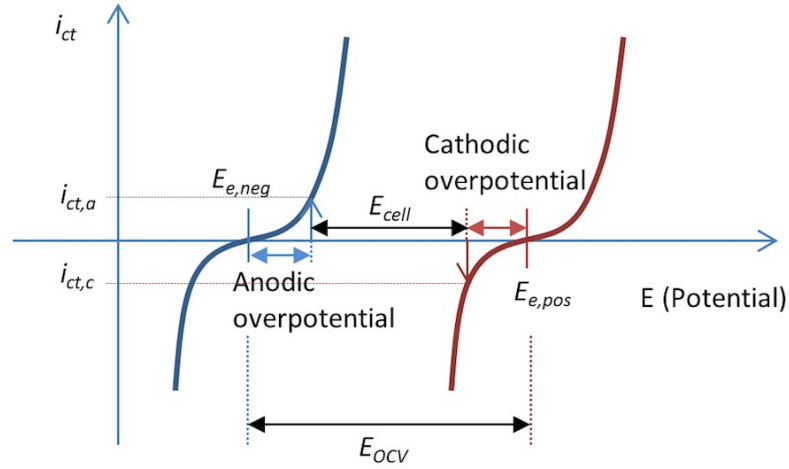
$$\eta = E - E_0$$

Fig: The charge transfer current density as a function of the electrode potential

for the anodic and cathodic over potential

4.2. Exchange current density (j_0):
The exchange current i_0 is the current in the absence of net electrolysis and at zero overpotential. The exchange current can be thought of as a background current to which the net current observed at various overpotentials is normalized. When exchange current is divided by area of electrode A exchange current becomes the exchange current density.

$$i_0 / A = j_0$$

4.3. Tafel slope (b):
The Tafel slope is the proportionality constant between the overpotential (η) and the logarithm of the current density ($\log j$) in the Tafel region of an electrochemical reaction. It reflects the kinetics of the rate-determining step and is typically expressed in millivolts per decade (mV/dec). A lower Tafel slope indicates faster reaction kinetics and higher catalytic efficiency.

$$\log(j) = \log(j_0) + \eta/b$$

$$\eta = a + b.\log(j)$$

$$b = \partial\eta/\partial\log(j) = 2.303RT/\alpha F$$

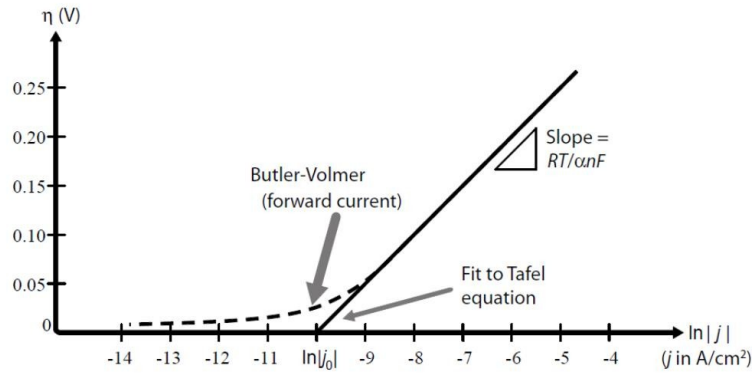Here α is the transfer coefficient.

Fig: overpotential as a function of exchange current density
for tafel like plot

4.4. Turnover frequency:
The turnover frequency (TOF) reflects the number of reaction products generated per active site per unit of time.It quantifies the intrinsic activity of a catalyst, independent of its mass or surface area.

$$TOF = mole(O_2, H_2 \text{ etc.}) / (mole \text{ of active sites} \times time (s))$$

4.5. Mass activity and Specific activity:
Mass activity of the catalysts are obtained by normalizing the current densities by the mass loading on the working electrode. However, OER is a surface reaction and only the atoms on the surface participate to the reaction. Other atoms underneath the surface do not contribute to the reaction. Hence, mass activity does not represent the intrinsic activity of the catalyst. A more accurate way to report the "true" activity of a catalyst is to normalize the current density by surface area to obtain a specific activity, as surface area can reflect the real number of active sites on the surface.

5. Oxide electrocatalysts for OER:

5.1. Pervoskite oxides:
Perovskite oxides have a general formula of ABO_3, where A-site cations are typically electropositive cations which are larger than B-site cations. B sites are typically occupied by transition metals or main group ions. A-site cations are in a 12-coordinate framework of corner-shared BO6 octahedra.

$$ABO_3 = (A_1)_{1-x}(A_2)_x(B_1)_{1-y}(B_2)_y O_3$$
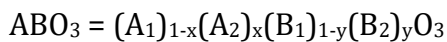
By creating different combinations of A and B sites we can modify valence state and electronic structure of the catalyst. It provides us some degree of freedom to tune crystal structure and also control the oxygen vacancy level. Feasibility of multimetal pervoskites is based on two parameters, Goldschmidt tolerance factor t and octahedral factor μ.

$$t = (r_A + r_O)/(\sqrt{2}\,(r_B + r_O))$$
$$\mu = r_B / r_O$$

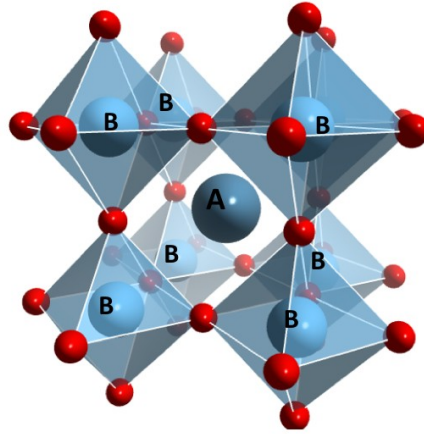r_A, r_B and r_O are the ionic radii for A site, B site and Oxygen.

Fig: Pervoskite type structure

$$A \ B \ O_3$$

$La^{3+}, Ce^{3+}, Nd^{3+}, Sm^{3+}, Eu^{3+}, Gd^{3+},$
$Tb^{3+}, Dy^{3+}, Ho^{3+}, Er^{3+}, Yb^{3+}, Lu^{3+}$

$Al^{3+}, Cr^{3+}, Fe^{3+}, Ga^{3+}, In^{3+}, Sc^{3+}$

For a stable pervoskite structure $0.8 <= t <= 1$, for $t = 1$ an ideal cubic structure, for $0.9 < t < 1$ cubic structure and for $0.8 < t < 0.9$ an orthorhombic or rhombohedral structure is formed. Except $0.8 <= t <= 1$, A is either too big or too small to be adjusted with BO_6 octahedron framework. μ should lie in the range of $0.44 < \mu < 0.72$ for a stable BO_6 octahedron to form.

5.2. Spinel Oxides:
Spinel oxides have a general formula of AB_2O_4, where A sites are typically charged as 2+ or sometimes 3+ at tetrahedral sites while B sites are charged as 3+ at octahedral sites.

$AB_2O_4 = (A_{1-\lambda}B_\lambda)_{Td}[A_\lambda B_{2-\lambda}]_{Oh}O_4$, $0 <= \lambda <= 1$

Tetrahedral block

Octahedral block

The unit cell built from alternate stacking of the A and B blocks.

Polyhedral model of the spinel unit cell showing the tetrahedra (green) and octahedra (blue) formed by the distorted cubic closest-packed oxygen (red).

The corner-sharing tetrahedral network (pyrochlore lattice) formed by the octahedral sites with the tetrahedral coordination of third nearest
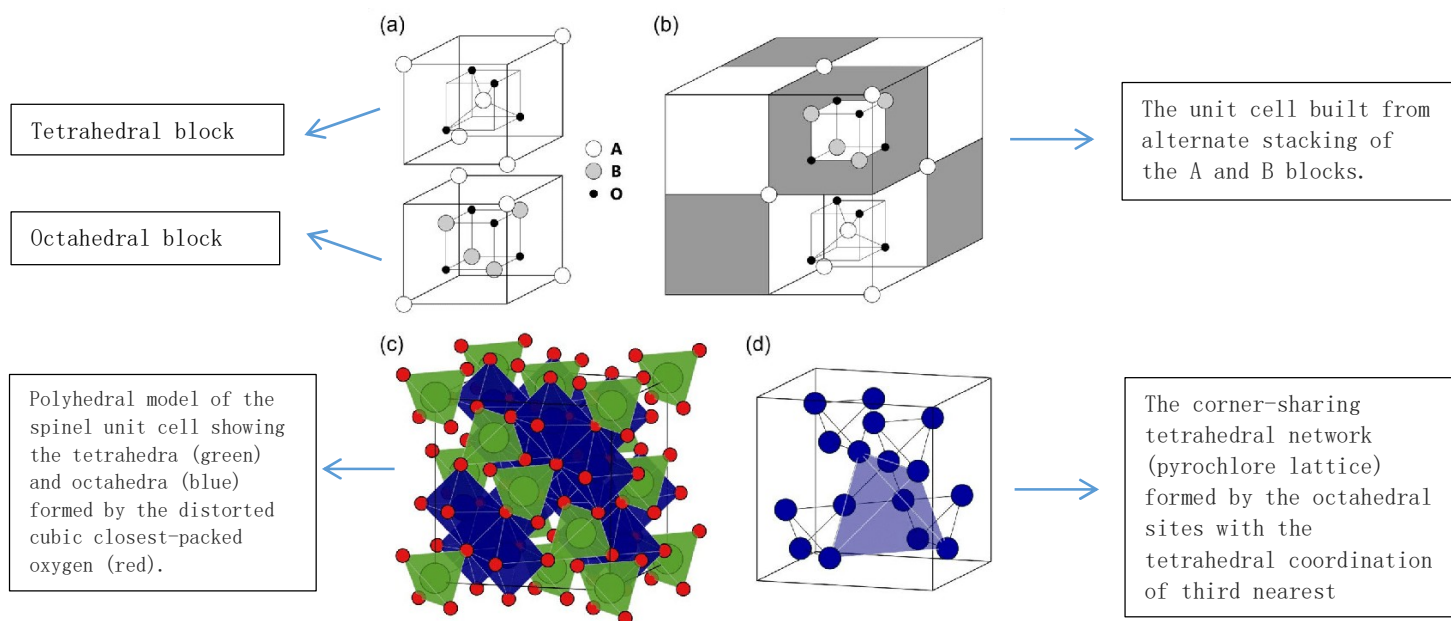
Fig: The spinel structure.

In the spinel structure depending on how cation occupy tetrahedral or octahedral sites, either normal or inversed spinel structure is formed. The parameter λ represents the degree of inversion in the spinel structure. When $\lambda = 0$ represents all the A^{2+} occupies the octahedral sites, while B^{3+} occupies tetrahedral sites. In the inverse spinel structure A^{2+} occupies octahedral sites and B^{3+} occupies partially octahedral and partially tetrahedral sites.

By modifying the M_{Td}-O and M_{Oh}-O bond lengths by metal cation substitution or doping, unit cell parameters and oxygen fractional coordinate can be changed. However, no influence on M_{Oh}-O bond lengths can be induced by substitution of tetrahedral cations. M_{Td} has a 43m symmetry with six equivalent unshared edges and no angular freedom. Cation substitution in Td site can only adjust the M_{Td}-O bond length. M_{Oh} has a 3m symmetry, with six unshared edges, pertaining to the faces perpendicular to the threefold axis, and six shared edges. The cation substitution in Oh site can modify the M_{Oh}-O bond lengths as well as the O-M_{Oh}-O angle. This altered O-M_{Oh}-O angle can further result in modified M_{Td}-O bond length.

5.3. Layered hydroxides:

Layered hydroxides have a general formula of $M^{2+}_{(1-x)}M^{3+}_{x}(OH)_2$, The metal cations stay in the octahedral site in a six-fold coordination. Most of the layered hydroxides exhibit hexagonal unit cell. The hydroxides with M^{2+}/M^{3+} ratio equal to 1 display an orthorhombic phase.
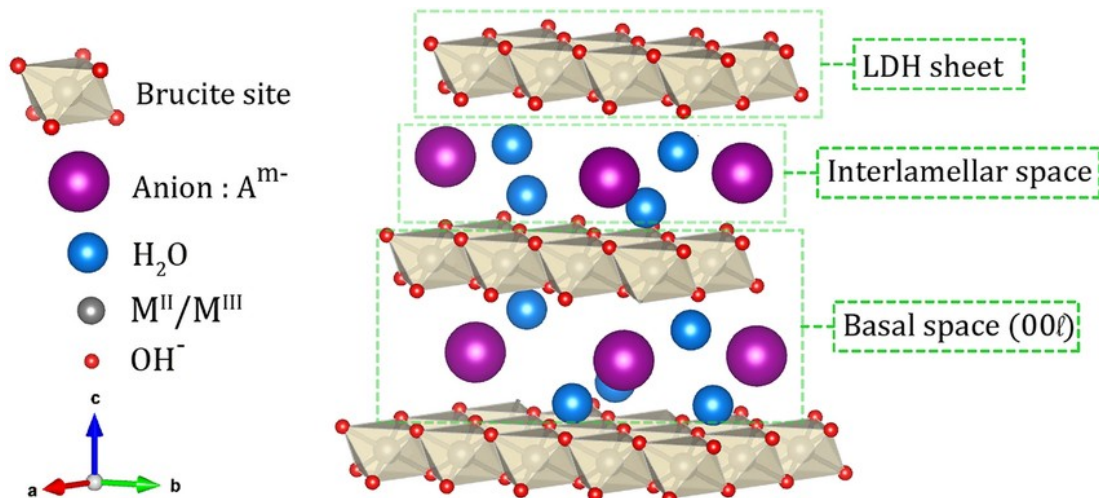
Fig: Layered double hydroxide structure

The crystal structure is a typical layered stacking conformation with proton H^+ sandwiching between layers, where the transition metals are located in the center of the octahedron with oxygen anions on the corners as [MO6] subunits and these subunits further connect to each other via sharing the edges to construct 2-D layers. Consequently, layer structure type oxides are classified as layered double hydroxides(LDH), and this family is usually cobalt and nickel based compounds because of their excellent activity toward OER. The structure of LDHs is derived from brucite, $Mg(OH)_2$, where magnesium ions are octahedrally coordinated with hydroxyl groups, forming stacked layers. In LDHs, partial substitution of divalent cations with trivalent ones introduces a positive charge to the layers, which is balanced by anions in the interlayer space. This interlayer region, hydrated by water molecules, is highly dynamic,

allowing for anion exchange. This structural flexibility enables LDHs to accommodate a wide variety of anions, from simple inorganic species to complex organic or biomolecular ions, making them highly versatile. The physicochemical properties of LDHs stem from their tunable composition and layered architecture. The metal cation ratio (M^{2+}/M^{3+}) can be adjusted to modify the layer charge, influencing the anion exchange capacity and interlayer spacing. The high surface area and porosity of LDHs, often enhanced through synthesis techniques which contribute to their efficacy in adsorption and catalysis. Additionally, LDHs exhibit a unique memory effect, where calcined LDHs (transformed into mixed metal oxides) can reconstruct their layered structure upon rehydration in the presence of anions, a property exploited in applications like pollutant removal and drug delivery.

Table 1 Important measurement and kinetic parameters for metal oxide electrocatalysts for OER

Catalysts	Electrolytes[a]	Substrate[a]	Overpotential (mV) at specific current density	Current density (mA cm^{-2}) at specific overpotential	Tafel slope (mV dec^{-1})	Ref.
Perovskite family						
$LaFeO_3$	1 M KOH	S. R.[b]	>900 @ 40 mA cm^{-2}	—	—	20
$La_{0.4}Sr_{0.6}FeO_3$	1 M KOH	S. R.[b]	622 @ 40 mA cm^{-2}	—	58	20
$La_{0.2}Sr_{0.8}FeO_3$	1 M KOH	S. R.[b]	502 @ 40 mA cm^{-2}	—	53	20
$SrFe_{0.8}Co_{0.2}O_3$	1 M KOH	S. R.[b]	507 @ 40 mA cm^{-2}	—	113	20
$SrFe_{0.5}Co_{0.5}O_3$	1 M KOH	S. R.[b]	412 @ 40 mA cm^{-2}	—	163	20
$La_{0.2}Sr_{0.8}Fe_{0.2}Co_{0.8}O_3$	1 M KOH	S. R.[b]	402 @ 40 mA cm^{-2}	—	80	20
$LaNiO_3$	1 M NaOH	S. R.[b]	—	13 @ 300 mV	43	21
$LaCoO_3$	1 M NaOH	S. R.[b]	—	1.6 @ 300 mV	70	21
$LaMnO_3$	1 M NaOH	S. R.[b]	—	0.05 @ 300 mV	126	21
$La_{0.8}Sr_{0.2}O_3$	1 M NaOH	S. R.[b]	—	0.03 @ 300 mV	200	21
$Ba_{0.5}Sr_{0.5}Co_{0.8}Fe_{0.2}O_{3-\delta}$	0.1 M KOH	GCE	250 @ 0.05 mA cm^{-2} 370 @ 10 mA cm^{-2}	—	—	22
$BaNi_{0.83}O_{2.5}$	0.1 M KOH	GCE	270 @ 0.05 mA cm^{-2}	—	—	124
$CaCu_3Fe_4O_{12}$	0.1 M KOH	GCE	400 @ 10 mA cm^{-2}	—	51	125
$CaFeO_3$	0.1 M KOH	GCE	390 @ 10 mA cm^{-2}	—	47	125
$SrFeO_3$	0.1 M KOH	GCE	410 @ 10 mA cm^{-2}	—	63	125
$LaFeO_3$	0.1 M KOH	GCE	500 @ 10 mA cm^{-2}	—	77	126
$La_{0.95}FeO_{3-\delta}$	0.1 M KOH	GCE	400 @ 10 mA cm^{-2}	—	48	126
Spinel family						
$MnFe_2O_4$	0.1 M KOH	GCE	470 @ 10 mA cm^{-2}	—	114	28
$CoFe_2O_4$	0.1 M KOH	GCE	370 @ 10 mA cm^{-2}	—	82	28
$NiFe_2O_4$	0.1 M KOH	GCE	440 @ 10 mA cm^{-2}	—	98	28
$CuFe_2O_4$	0.1 M KOH	GCE	410 @ 10 mA cm^{-2}	—	94	28
Fe_3O_4	1 M KOH	Ni	—	0.2 @ 650 mV	43	130
$Ni_{0.5}Fe_{2.5}O_4$	1 M KOH	Ni	—	0.31 @ 650 mV	35	130
$NiFe_2O_4$	1 M KOH	Ni	—	0.62 @ 650 mV	42	130
Mn_3O_4	1 M KOH	GCE	>600 @ 3 mA cm^{-2}	—	60	132
$Mn_{2.4}Co_{0.6}O_4$	1 M KOH	GCE	510 @ 3 mA cm^{-2}	—	51	132
$Mn_{2.1}Co_{0.9}O_4$	1 M KOH	GCE	490 @ 3 mA cm^{-2}	—	31	132
Co_3O_4	1 M KOH	Au	400 @ 10 mA cm^{-2}	—	49	133
Co_3O_4 nanooctahedron	0.1 M KOH	GCE	530 @ 10 mA cm^{-2}	—	60	134
Co_3O_4 nanocube	0.1 M KOH	GCE	580 @ 10 mA cm^{-2}	—	60	134
$CoCr_2O_4$	1 M KOH	GCE	422 @ 10 mA cm^{-2}	—	63.3	135
$CoCr_2O_4/CNT$	1 M KOH	GCE	326 @ 10 mA cm^{-2}	—	51	135
Layer-structure type family						
$MnOOH$	0.1 M KOH/LiOH	PtO/AuO	550 @ 5 mA cm^{-2}	—	—	27
$FeOOH$	0.1 M KOH/LiOH	PtO/AuO	525 @ 5 mA cm^{-2}	—	—	27
$CoOOH$	0.1 M KOH/LiOH	PtO/AuO	450 @ 5 mA cm^{-2}	—	—	27
$NiOOH$	0.1 M KOH/LiOH	PtO/AuO	375 @ 5 mA cm^{-2}	—	—	27
γ-$NiOOH$	0.1 M KOH	Au	700 @ 10 mA cm^{-2}	—	—	141
γ-$Ni_{0.87}Fe_{0.13}OOH$	0.1 M KOH	Au	390 @ 10 mA cm^{-2}	—	—	141
γ-$Ni_{0.75}Fe_{0.25}OOH$	0.1 M KOH	Au	370 @ 10 mA cm^{-2}	—	—	141
NiFe-LDH	1 M KOH	GCE	300 @ 10 mA cm^{-2}	—	40	31
NiCo-LDH	1 M KOH	GCE	335 @ 10 mA cm^{-2}	—	41	31
CoCo-LDH	1 M KOH	GCE	350 @ 10 mA cm^{-2}	—	45	31
FeNi–rGO LDH	1 M KOH	Ni foam	195 @ 10 mA cm^{-2}	—	39	145
FeNi–GO LDH	1 M KOH	Ni foam	210 @ 10 mA cm^{-2}	—	40	145
NiCr DH	0.1 M KOH	Au	310 @ 1 mA cm^{-2}	—	—	147
NiMn DH	0.1 M KOH	Au	380 @ 1 mA cm^{-2}	—	—	147
NiFe DH	0.1 M KOH	Au	290 @ 1 mA cm^{-2}	—	—	147
NiCo DH	0.1 M KOH	Au	500 @ 1 mA cm^{-2}	—	—	147
$Ni(OH)_2$	0.1 M KOH	Au	410 @ 1 mA cm^{-2}	—	—	147
NiCu DH	0.1 M KOH	Au	450 @ 1 mA cm^{-2}	—	—	147
NiZn DH	0.1 M KOH	Au	>500 @ 1 mA cm^{-2}	—	—	147
$LiCoO_2$	0.1 M KOH	CFP	>520 @ 5 mA cm^{-2}	—	48	30

De-LiCoO$_2$	0.1 M KOH	CFP	380 @ 5 mA cm^{-2}	—	50	30
De-LiCo$_{0.5}$Ni$_{0.5}$O$_2$	0.1 M KOH	CFP	370 @ 5 mA cm^{-2}	—	42	30
De-LiCo$_{0.5}$Fe$_{0.5}$O$_2$	0.1 M KOH	CFP	335 @ 5 mA cm^{-2}	—	40	30
De-LiCo$_{0.33}$Ni$_{0.33}$Fe$_{0.33}$O$_2$	0.1 M KOH	CFP	295 @ 5 mA cm^{-2}	—	48	30
De-LiCo$_{0.33}$Ni$_{0.33}$Mn$_{0.33}$O$_2$	0.1 M KOH	CFP	395 @ 5 mA cm^{-2}	—	46	30
Other oxides						
a-Fe$_{36}$Co$_{64}$O$_x$	0.1 M KOH	FTO	270 @ 1 mA cm^{-2}	—	40	153
a-Fe$_{40}$Ni$_{60}$O$_x$	0.1 M KOH	FTO	250 @ 1 mA cm^{-2}	—	34	153
a-Fe$_{40}$Co$_{39}$Ni$_{22}$O$_x$	0.1 M KOH	FTO	280 @ 1 mA cm^{-2}	—	40	153
a-Co$_{41}$Ni$_{59}$O$_x$	0.1 M KOH	FTO	270 @ 1 mA cm^{-2}	—	73	153
CoPi	0.1 M KPi	ITO	410 @ 1 mA cm^{-2}	—	62	32
MnO$_x$	0.10 M Pi and 1.73 M KNO$_3$	FTO	$\sim$460 mV @ 0.01 mA cm^{-2}	—	127	39
Ni–Bi	0.5 M KB(OH)$_4$, H$_3$BO$_3$, 1.75 M KNO$_3$	FTO	380 mV @ 1 mA cm^{-2}	—	29	162
Bi$_2$WO$_6$ CNP concave nanoplates	0.5 M Na$_2$SO$_4$	GCE	540 mV @ 1 mA cm^{-2}	—	—	37
Mn$_5$O$_8$ NPs	0.3 M phosphate buffer solution	FTO	580 mV @ 5 mA cm^{-2}	—	78.7	34
Co(PO$_3$)$_2$	0.1 M phosphate (NaH$_2$PO$_4$, Na$_2$HPO$_4$)	GCE	440 mV @ 8 mA cm^{-2}	—	74.1	158

[a] For the samples in the same work the electrolyte and substrate only stated in the first sample have been used for the sake of clarity. [b] Sintered rod sample.

6. Conclusion and Future Perspectives:

The Oxygen Evolution Reaction (OER) plays a crucial role in the move toward cleaner and more sustainable energy sources. It's a key part of technologies like water splitting, which can help us produce hydrogen-one of the cleanest fuels available. But while the science behind it is promising, the slow speed of OER compared to other reactions (like hydrogen evolution) remains a big challenge. This slow pace is mainly due to the complex nature of the reaction, which involves multiple steps and requires a lot of energy to get going.

To address this, researchers have turned to a wide range of electrocatalysts especially transition metal based oxides and hydroxides such as perovskites, spinels, and layered double hydroxides (LDHs). These materials show great promise because they are relatively stable, tunable, and made from earth-abundant elements. Over the years, scientists have developed several ways to measure and compare the performance of these catalysts-focusing on things like overpotential, Tafel slope, and turnover frequency.

What's becoming clear is that the structure and composition of these materials play a major role in how well they work. Subtle changes in their crystal structure, the presence of oxygen vacancies, or the mix of metal ions can significantly improve their efficiency. That's exciting because it means we can design better catalysts by understanding the relationships between their structure and their performance.

Looking to the future, there's still a lot to explore. We need deeper insight into what's really happening at the atomic level during the reaction. Tools that let us watch the reaction in real time-like in-situ spectroscopy-could help uncover the true nature of the active sites. On the computational side, machine learning and advanced simulations can speed up the search for new materials by predicting what works best before we even make it in the lab.

At the same time, we'll need to focus on making these catalysts durable and scalable for real-world use. That means using low-cost, abundant materials that can work over long periods without breaking down. We should also think about hybrid systems-materials that can perform more than one function, like both OER and HER, in different environments.

In short, while we've made significant progress in understanding and improving OER catalysts, there's still a long road ahead. But with collaborative efforts across chemistry, materials science, and engineering, we're steadily moving toward a future powered by clean, sustainable, and efficient energy solutions.

7. Abbreviations:

OER	Oxygen evolution reaction
CFP	Carbon fiber paper
HER	Hydrogen evolution reaction
LDH	Layered double hydroxides
NP	Nanoparticle
NS	Nanosheet
DFT	Density Functional Theory
CV	Cyclic Voltammetry
CP	Chronopotentiometry
CA	Chronoamperometry
TOF	Turnover Frequency
ECSA	Electrochemically active surface area

8. Acknowledgements:

9. Refrences:

1. Nian-Tzu Suen, Sung-Fu Hung, Quan Quan, Nan Zhang, Yi-Jun Xu and Hao Ming Chen, *Chem. Soc. Rev., 2017, **46**, 337*

2. S. Anantharaj, S.R.Ede, K. Karthick, S. Sam Sankar, K. Sangeetha, P.E. Karthik and Surata Kundu, *Energy Environ. Sci., 2018, **11**, 744*

3. HongminvAn, Wonchul Park, Heejong Shin, Dong Young Chung, *EcoMat., 2024, **6**, 10*

4. Qiuhua Liang, Geert Brocks and Anja Bieberle-Hütter, *J. Phys. Energy, 2021, **3**, 026001*